Selection and Performance of AM Superalloys for High-Speed Flight Environments

William Sean James (w.james@cranfield.ac.uk)
Cranfield University https://orcid.org/0000-0001-9780-8396
Supriyo Ganguly
Goncalo Pardal

Research Article

Keywords: Additive manufacturing, Alloy selection, Mechanical properties, Rene 41, Inconel 718, Haynes 188, Inconel 625

Posted Date: July 15th, 2022

DOI: https://doi.org/10.21203/rs.3.rs-1666707/v1

Version of Record: A version of this preprint was published at The International Journal of Advanced Manufacturing Technology on September 1st, 2022. See the published version at https://doi.org/10.1007/s00170-022-10005-9.

Abstract

In developing the Wire + Arc Additive Manufacturing (WAAM) process for the manufacture of components used in high-speed flight environments, a selection process for suitable alloys was devised. Using elevated temperature material properties from literature sources, creep-resistant alloys were down selected based on the requirement for service in a high temperature, high stress environment and the need for an alloy suitable for additive manufacturing using a wire-arc process. Down selected alloys Inconel 718 (IN718), Rene 41 (RE41), Haynes 188 (H188) and Inconel 625 (IN625) were deposited by a plasma transferred arc WAAM process in an oxygen-controlled environment. The structures were built then underwent mechanical testing. The performance of as deposited material was then compared against wrought alloy data from literature.

Tensile testing at room temperature revealed a correlation with similarly strengthened IN718 & RE41, but no correlation with solution strengthened H188 and IN625. Results revealed that the AM material did not meet the wrought strength and with performance varying depending on each alloy's strengthening mechanism. Results illustrate the need for further processing to return the mechanical performance to wrought values.

1 Introduction

In this paper 73 alloys are ranked against the application of a structural component in a high-speed flight environment of short duration (< 1 hour), where the external structural component could reach service temperatures of 1200 + K. Components for such an application will also be highly stressed to minimise structural mass.

The only group of alloys suitable for this application are creep-resistant superalloys, which are predominantly alloys intended for service at high temperatures which often contain high volumes of Ni and Cr, with a base element other than Fe [1]. The alloys investigated in this study are Ni-based and Co-based superalloys. These materials are alloyed specifically with Cr to offer oxidisation resistance which is obtained through the formation of oxide scale Cr_2O_3 at the component's surface. Traditionally these alloys have included Ni, Fe, and Co based superalloys, which have been specifically developed for high temperature applications and often boast significant retention of mechanical strength at elevated temperatures and low surface deformation. These alloys often feature a primary an austenitic, face-centred-cubic (fcc) matrix, and an array of secondary strengthening phases and carbides to enhance creep resistance. Fe-Ni based alloys are strengthened by precipitation of intermetallic compounds within the matrix, most commonly by γ' precipitates, but can also be solid-solution strengthened. Ni based superalloys are mostly strengthened by the precipitation of intermetallic compounds in an austenitic fcc matrix. When Ti and Al are included in the composition, γ' is often the strengthening precipitate. For alloys including Nb, γ" is also a strengthening precipitate. Ni based alloys can also be solid solution strengthened but this is less common. Some Ni alloys, called oxide-dispersion-strengthened alloys, are strengthened by the inclusion of inert particles in the matrix. Co based alloys are usually strengthened by both solid solution strengthening and carbides. [2][3]

An investigation into the effects that the Wire + Arc Additive Manufacturing (WAAM) process has on these alloys was also required, to ensure no adverse effects on the material properties. The WAAM process uses welding power sources and wire as a feedstock to deposit material in a layer-by-layer process [4]. Due to the repetitive layer-by-layer process, WAAM components also undergo a successive heating and cooling cycle which would significantly affect the metallurgical response of an alloy.

A large volume of literature exists on alloy selection for a huge variety of applications, each selection method is dependent on application and what the intended use is. This selection process is somewhat different in considering not only end application but also in selecting alloys suitable for the manufacturing process, in this case WAAM.

2 Method

2.1 Alloy Selection

An analysis of existing data found in literature was utilised for the purpose of ranking alloys against the application criteria. Several comprehensive sources of data were utilised for this purpose:

- Metallic Materials Properties Development and Standardization (MMPDS-12) [1]
- Superalloys - A Technical Guide by Donachie, M. J. and Donachie S. J. [5]
- Materials Properties Database for Selection of High-Temperature Alloys and Concepts of Alloy Design for SOFC Applications [6]
- High-Temperature High-Strength Nickel-Base Alloys No. 393, Nickel Institute [7]

In addition, respective manufacturer data sheets were utilised, and in some cases where data was otherwise unavailable, properties were estimated via both interpolation and extrapolation depending on the missing value (estimated figures are indicated in the Appendix).

73 alloys were considered, and each alloy was scored against the chosen criteria, where the highest score indicates the most appropriate choice, and the lowest score indicates the least appropriate alloy. Each alloy was ranked in each category out of a possible maximum of 73. The score from each category was then totalled to give a final rank. The scoring formula is comprised of a series of simplified equations intended to easily identify potentially suitable alloys amongst an extensive list. An example of the mechanical data extracted from literature is included in Fig. 1.

The scoring formula is as follows:

Equation 1 Scoring formular for alloy ranking system.

$$R_{Total} = R.UTS_{1000} + R.UTS_{1400} + R.YS_{1000} + R.YS_{1400} + R.\eta_{W_{1000}} + R.\eta_{W_{1400}} + R.\eta_{B_{1000}} + R.\alpha_{1000} + R.E_{1000} + R.(\alpha \bullet E)_{1000} + R.s$$

$R.X_T$ Where R indicates ranked position, X is representing the category (UTS for example) and T is the temperature in °F. UTS is the ultimate tensile strength, YS is the yield strength, α is the coefficient of thermal expansion, E is the dynamic modulus of elasticity.

Weight efficiency (η_W) also known as specific strength is given by:

Equation 2 Weight efficiency.

$$\eta_W = \frac{UTS}{\rho}$$

Buckling efficiency (η_B) is given by:

Equation 3 Buckling efficiency.

$$\eta_B = \frac{E^{0.5}}{\rho}$$

Susceptibility to post weld heat treat (PWHT) cracking (s) is given by:

Equation 4 Susceptibility to PWHT cracking.

$$s = \frac{|k + mx_0 - y_0|}{\sqrt{1+m^2}} = \frac{|4.5 - Ti_{\%wt} - Al_{\%wt}|}{\sqrt{2}}$$

The equation of the line in Fig. 2 is given by $y = mx + k$ and the coordinate of each point is given as (x_0, y_0). The susceptibility to PWHT in Eq. 4 above, is a calculation based on Ti and Al content of each alloy and is the distance of the points on Fig. 2 from the 'increased strain-age cracking' line indicating the max. content while remaining within the weldable zone. A lower value in this category represents alloys which are closer to the line, indicating better suitability. Alloys that were significantly above the 'increased strain-age cracking' line were excluded from selection.

To select alloys for mechanical testing, the top performing alloy from the alloy selection process, RE41, was down selected. IN718 was also selected as the alloy has been the subject of previous research using WAAM and is included for comparative purposes due to the alloy having larger volumes of data existing in the literature. H188 was selected to better understand the performance of cobalt-based alloys manufactured using the WAAM system, and IN625 as a solid solution strengthened Ni-base alloy.

2.2 WAAM Deposition

The selected alloys were deposited using a WAAM system consisting of a FANUC six-axis robotic arm, a plasma water-cooled welding torch mounted to the robotic arm, a wire feeder, and a part-rotator - which allowed for WAAM walls to be built on both sides of the substrate plate.

The WAAM deposition process took place inside of an inert enclosure, which provided an Argon atmosphere of less than 800 ppm of oxygen and was monitored using an oxygen analyser. The experimental set-up is shown in Fig. 3.

Wall structures were deposited from commercially available wires on both sides of a 10 mm thick Inconel 718 substrate plate. The composition of the welding wires is given in Table 1 and welding parameters in Table 2.

Table 1
Composition of welding wires. (% weight)

Inconel 718													
Ni	Cr	Fe	Nb	Mo	Ti	Al	Mn	Si	Cu	C	Others		
53.57	18.56	17.8	5.01	2.87	0.97	0.60	0.10	0.08	0.07	0.04	0.51		
Rene 41													
Ni	Cr	Co	Mo	Ti	Fe	Al	Nb	V	Si	C	Cu	Mn	Others
53.7	18.9	10.2	9.08	3.20	2.72	1.64	0.12	0.12	0.09	0.07	0.04	0.03	0.007
Haynes 188													
Co	Ni	Cr	W	Fe	Mn	Si	C	La	P	Others			
37.12	22.90	22.20	13.90	2.65	0.81	0.22	0.107	0.06	0.011	0.005			
Inconel 625													
Ni	Cr	Mo	Nb	Fe	Ti	Al	Si	Cu	Mn	C	Others		
64.75	22.16	8.79	3.60	0.24	0.19	0.17	0.04	0.02	0.02	0.01	0.006		

Table 2
Welding parameters.

	IN718	RE41	H188	IN625
Wire Diameter (mm)	1.2	1	1.14	1.2
Torch to work distance (mm)	8	8	8	8
Current (A)	180	180	180	180
Wire feed speed (m/min)	1.8	2.4	2	1.8
Travel speed (m/min)	0.3	0.36	0.36	0.3
Inter-pass temperature (°C)	170	170	170	170

2.3 Mechanical Testing

For each selected alloy to undergo tensile testing, samples were extracted from the WAAM walls and machined into coupons. The room temperature (RT) coupon, conforming to ASTM E8(M) sub-size specification, is shown in Fig. 4. Three coupons were tested from each alloy in the build height orientation (vertical direction). Samples were tested at RT, using an Instron 8801 Servo hydraulic Universal Testing System, and tested to failure using ASTM E8(M). Tensile tests used a strain rate of 0.005 min^{-1} until the onset of plastic deformation and thereafter a crosshead speed of 1.6 mm/min. Specimens were extracted from similar locations on the WAAM wall to minimise variation caused by the WAAM aging effect.

3 Results

3.1 Alloy Selection

The top five alloys and their score in each category are given in Table 3, as well as the scores of each of the selected alloys (RE41, IN718, H188, IN625).

Table 3
Ranking of alloys.

Designation	Total Score	UTS		YS		η_W		η_B	α	E	Stress (α·E)	Cracking
		1000 F	1400 F	1000 F	1400 F	1000 F	1400 F	1000 F	1000 F	1000 F		
Rene 41	673	67	66	63	66	68	66	41	65	37	64	70
MP159	608	71	70	72	72	71	71	35	25	51	15	55
MP35N	593	72	72	71	71	73	73	54	25	72	8	(2)
M-252	591	56	58	46	51	57	57	36	69	30	68	63
Inconel 617	567	19	42	19	25	21	43	48	111	64	111	64
Inconel 718	560	61	59	66	54	61	59	26	50	26	57	41
Inconel 625	314	36	30	26	29	35	31	24	20	37	18	28
Haynes 188	280	25	37	20	23	22	35	1	37	22	56	(2)

As can been seen in Table 3 there is not a significant difference in total score between most of the alloys presented. Alloys MP159 and H188 could not be ranked in the susceptibility to cracking category due to both alloys lacking Al and Ti in their composition. In fact, little to no cracking was visually observed in H188 samples.

3.2 Mechanical Testing

The results of tensile testing are given in Table 4 and Fig. 5, where wrought (Wro) values are presented alongside testing results for AD samples. The data shows a mismatch with the wrought data from literature, with AD samples performing someway behind the wrought values. The best UTS performance was achieved by RE41 where the performance was 72% of the wrought value, followed by H188, IN625 and IN718, which achieved 69, 64 and 54% of the wrought values respectively. Comparing the YS performance there is a correlation between the performance of solid solution strengthened alloys and the precipitation strengthened alloys. H188, IN625, RE41 and IN718 achieved 85, 81, 72, and 41% of the wrought YS respectively.

Table 4
RT Mechanical results, and comparison with wrought (Wro) literature data [9].

Alloy	Condition	UTS (MPa)	0.2 & YS (MPa)	Elongation (%)
IN718	Wro	1435	1185	21
	AD	774.30	485.33	23.90
RE41	Wro	1420	1060	14
	AD	1017.40	764.00	26.16
H188	Wro	960	485	56
	AD	660.89	412.00	56.26
IN625	Wro	965	490	50
	AD	622.21	396.97	57.26

The difference in performance between the alloys could be explained by the differences is strengthening mechanisms. For example, IN718 undergoes an extensive aging process to achieve maximum strength, whereas RE41 although also precipitation strengthen typically undergoes a less extensive treatment, H188 and IN625 are both primarily solid solution strengthened, which helps to explain why the performance of these alloys more closely resembles the wrought values.

4 Discussion

The alloy ranking method, although basic, provides an insight into the performance of the alloys in relation to the application. For the high-speed flight environment, performance at elevated temperature such as strength, weight efficiency, and elongation are important factors. The ranking formula (Eq. 1) naturally weights more importance on the alloy's strength, by having the UTS and YS input into the equation in five separate terms in total, including weight efficiency (specific strength) where UTS is also a term. Although strength is a large factor in the ranking formula, it does include several other factors which are important for high-speed flight, such as density which will affect the overall weight of any components. Elastic modulus and coefficient of thermal expansion are also used on the basis that they will largely dictate the deformation and corresponding thermal stress that any component will experience under high level of service loading at an elevated temperature. Finally, components are ranked using on their suitability for welding, which eliminates any alloys that would experience a large degree of strain age cracking as a result of welding. The volume of Ti and Al in the matrix of precipitation-hardened alloys is a factor in how susceptible the alloy will be to strain-age cracking. As the alloys are effectively heated at and beyond their aging temperature during deposition, they precipitate γ' particles during the process affecting the ductility during the process [8]. Interestingly, six of the studied alloys were eliminated due to weldability concerns that otherwise would have appeared within the top 10. This indicates that the majority of superalloys with high strength at temperature are both susceptible to cracking during welding and contain high volumes of Al and/or Ti. To further understand the affect the WAAM process has on the microstructure and fracture methods, this will be the subject of a future article.

To increase the strength of the alloys further an inter-pass cold working process could be included in the WAAM process, which will be investigated in a future article. A previous study by Xu et al found that cold rolling IN718 after each layer deposited increased the strength to meet and in some cases exceed the wrought performance [10]. The difference observed between the AD samples and the wrought strength highlights the need for additional processing of the alloys such as post-process heat-treatments and/or mechanical working to return to wrought performance. Precipitation of secondary phases at the grain boundary are one of the main sources of strength for precipitation strengthened alloys. In a previous study on IN718 by Xu et al, it was suggested that the presents of large columnar grains in the WAAM structure make the precipitation of these phases less likely, due to the reduced grain boundary area [11]. This makes the use of a mechanical process to disrupt the large WAAM grains a necessity to achieve peak strength.

Further research is required to establish processing methods which can return WAAM deposited creep resistant alloys to their wrought performance.

5 Conclusions

In conclusion, alloys were identified for the high-speed flight application based on existing literature data using a scoring formula of material properties and simplified equations. The selected alloys then underwent mechanical testing after WAAM deposition to understand the effect on the alloys when compared with the wrought data from the literature.

The study found:

1. Alloy RE41 is the most suitable alloy for both WAAM deposition and for application in high temperature - high stress environments.

2. Mechanical testing shows a correlation between RE41 and IN718 with similar strengthening mechanisms but no correlation with H188 and IN625.

3. AD WAAM alloys IN718, RE41, H188 and IN625 are significantly weaker than the wrought material and the difference is largely dictated by the strengthening mechanism.

4. WAAM deposition of solid solution strengthened alloys, H188 and IN625 achieves YS performance closer to wrought values.

5. Additional investigation is required into methods of returning WAAM superalloys to their wrought strength.

Declarations

6 ACKNOWLEDGMENTS

The authors wish to acknowledge the UK Ministry of Defence for their financial support, and the industrial supervisors from DSTL Porton Down, for their ongoing advice and guidance: Mr Graham Simpson, Dr Sarah Baker and Dr Matthew Lunt.

The authors would also like to acknowledge the assistance from welding technicians Mr Flemming Nielsen, Mr Nisar Shah, and Lab manager Mr John Thrower, without whom this work would not have been possible.

7 STATEMENTS & DECLARATIONS

a. This work was funded by the Defence Science & Technology Laboratory, UK (DSTL)

b. The authors have no relevant financial or non-financial interests to disclose.

c. The raw/processed data required to reproduce these findings cannot be shared at this time as the data also forms part of an ongoing study.

d. Code availability: *Not applicable*

e. In the author's opinion there are no ethical issues with the research presented in this paper. The authors confirm this manuscript has not been published elsewhere and is not under consideration by another journal.

f. Consent to participate: *Not applicable*

g. All authors consent to the publication of this paper.

References

1. Battelle Memorial Institute (2017) 'Heat-Resistant Alloys', in *Metallic Materials Properties Development and Standardization (MMPDS-12)*. Battelle Memorial Institute. Available at: https://app.knovel.com/hotlink/pdf/id:kt00CX2NX1/metallic-materials-properties/metallic-m-mechanical
2. Donachie MJ, Donachie SJ (2002) 'Understanding Superalloy Metallurgy'. Superalloys - A Technical Guide, 2nd edn. ASM International, pp 25–39. doi: 10.31399/asm.tb.stg2.t61280025.
3. Yang Z, Weil KS, Paxton DM, Stevenson JW (2003) 'Selection and Evaluation of Heat-Resistant Alloys for SOFC Interconnect Applications'. J Electrochem Soc 150(9):A1188. doi: 10.1149/1.1595659
4. Xu X, Ganguly S, Ding J, Guo S, Williams S, Martina F(2018) 'Microstructural evolution and mechanical properties of maraging steel produced by wire + arc additive manufacture process', *Materials Characterization*. Elsevier, 143(November 2017), pp. 152–162. doi: 10.1016/j.matchar.2017.12.002
5. Donachie MJ, Donachie SJ(2002) *Superalloys - A Technical Guide*. 2nd edn. ASM International. Available at: https://app.knovel.com/hotlink/toc/id:kpSATGE003/superalloys-technical/superalloys-technical
6. Yang ZG, Stevenson JW, Paxton DM, Singh P, Weil KS (2002) Materials Properties Database for Selection of High-Temperature Alloys and Concepts of Alloy Design for SOFC Applications. Pac Northwest Natl Lab. doi:10.2172/15010553
7. INCO (2020) *High-Temperature High-Strength Nickel-Base Alloys No. 393*. Available at: https://nickelinstitute.org/media/8d93486143182f5/nickel_incopub393_updated-june-2021.pdf
8. Donachie MJ, Donachie SJ(2002) 'Joining Technology and Practice', in *Superalloys - A Technical Guide*. 2nd edn. ASM International, pp. 65–78. Available at: https://app.knovel.com/hotlink/pdf/id:kt008GQY5K/superalloys-technical/joining-superalloys
9. Donachie MJ, Donachie SJ(2002) 'Selection of Superalloys', in *Superalloys - A Technical Guide*. 2nd edn. ASM International, pp. 11–24. Available at: https://app.knovel.com/hotlink/pdf/id:kt008GQQU1/superalloys-technical/superalloy-forms
10. Xu X, Ganguly S, Ding J, Seow CE, Williams S (2018) 'Enhancing mechanical properties of wire + arc additively manufactured INCONEL 718 superalloy through in-process thermomechanical processing'. Materials and Design, vol 160. Elsevier Ltd, pp 1042–1051. doi: 10.1016/j.matdes.2018.10.038.
11. Xu X, Ding J, Ganguly S, Williams S(2019) 'Investigation of process factors affecting mechanical properties of INCONEL 718 superalloy in wire + arc additive manufacture process', *Journal of Materials Processing Technology*. Elsevier, 265(September 2018), pp. 201–209. doi: 10.1016/j.jmatprotec.2018.10.023

Appendix

APPENDIX: SAMPLE OF MECHANICAL PROPERTIES FROM LITERATURE

Designation	Score	Form	Density	UTS (MPa)			YS (MPa)			Tensile elongation (%)		
			kg/m^3	21°C	538 °C	760 °C	21°C	538 °C	760 °C	21°C	538 °C	760 °C
Nickel base												
Inconel 617	260	Bar	8360	740	580	440	295	200	180	70	68	84
Inconel 625	304	-	8440[7]	965	910	550	490	415	415	50	50	45
Inconel 718	557	Bar	8220	1435	1275	950	1185	1065	740	21	18	25
M-252	587	Bar	8250	1240	1230	945	840	765	720	16	15	10
Rene 41	703	Bar	8250	1420	1400	1105	1060	1020	940	14	14	11
Cobalt base												
Haynes 188	280	Sheet	8980	960	740	635	485	305	290	56	70	43
MP35N	588	Bar	8410	2025	(1773)	(1548)	1620	(1430)	(1415)	10	-	-
MP159	594	Bar	8330*	1895	1565	(1340)	1825	1495	(1480)	8	8	-

Designation	Mean coefficient of thermal expansion α (10^{-6} K)	Dynamic modulus of elasticity E		Content (%wt)	
	538 °C	21 °C	538 °C	Al	Ti
Nickel base					
Inconel 617	13.9	210	176	1	0
Inconel 625	15.3[6]	208[7]	179[7]	0.2	0.2
Inconel 718	14.4	200	171	0.5	0.9
M-252	13.0	206	177	1	2.6
Rene 41	13.5	220[7]	191[7]	1.5	3.1
Cobalt base					
Haynes 188	14.8	207	192[7]	0	0
MP35N	(15.3)	231	(192)	0	0
MP159	15.1[7]	206[7]	(167)	0.2	3

Data from Donachie Superalloys – A Technical Guide [9], unless otherwise specified.
* Manufacturers data

(Extrapolated/ interpolated values are shown in parentheses)

Figures

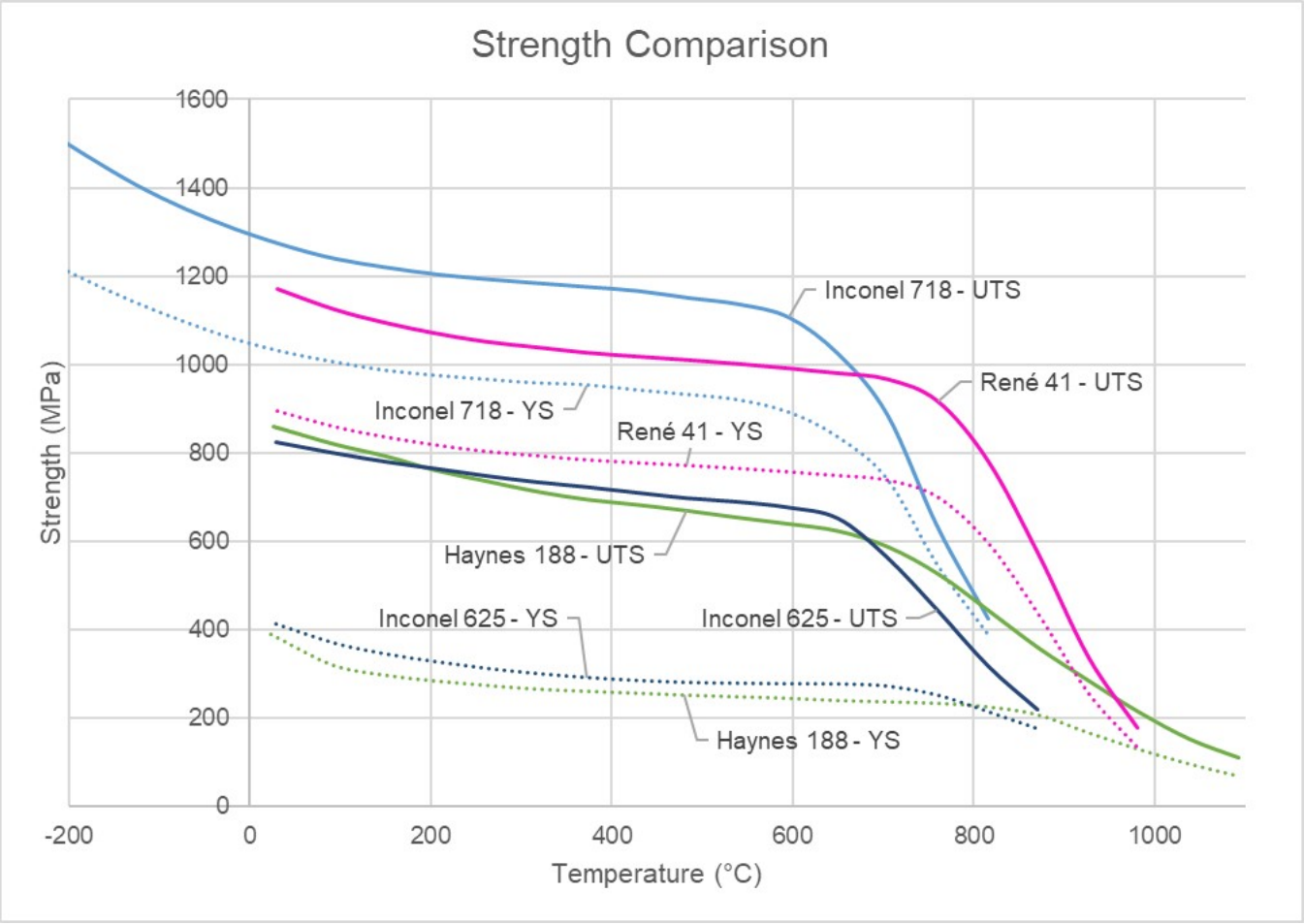

Figure 1

Literature data of alloy strength at temperature. [1]

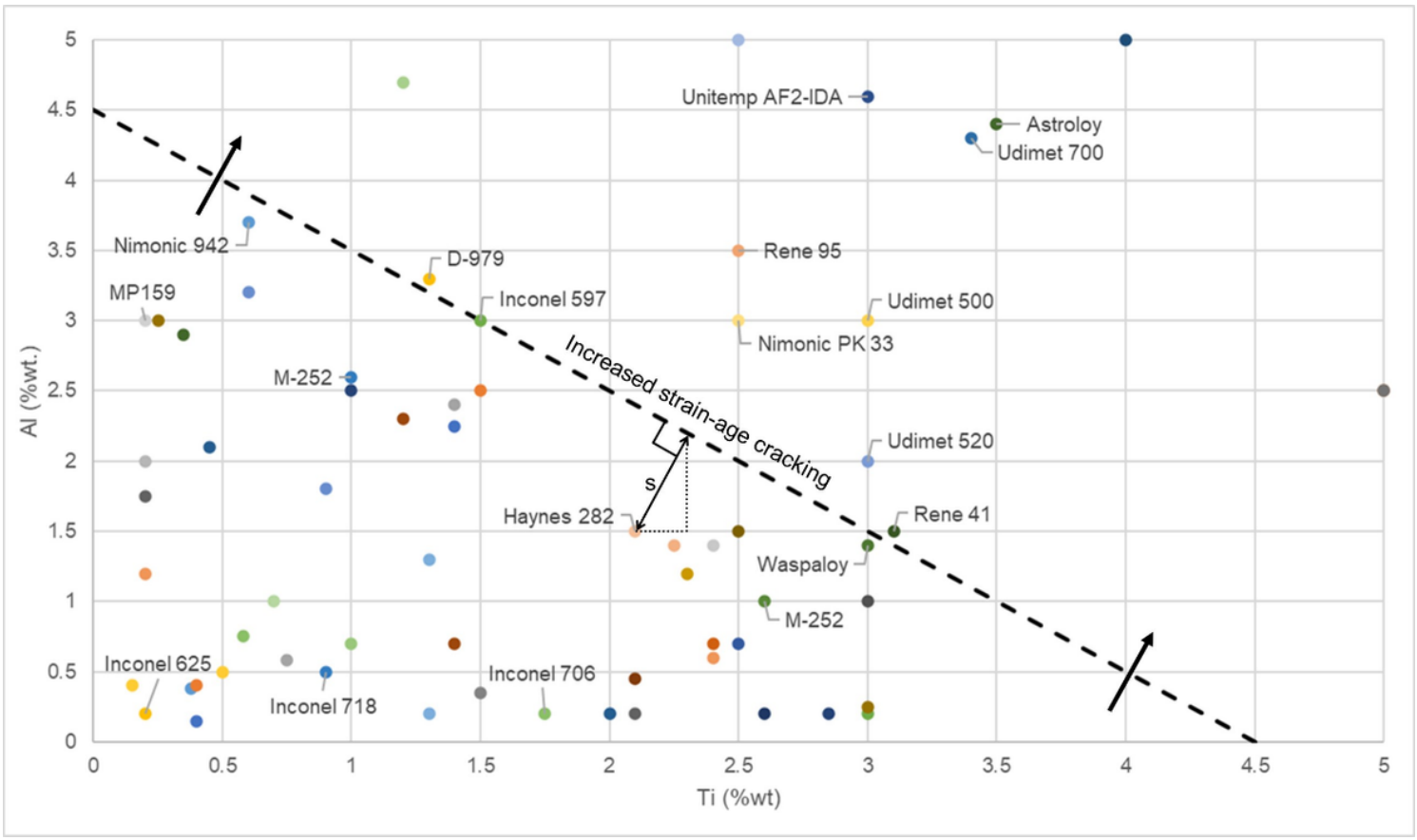

Figure 2

Diagram of Ti and Al content illustrating weldability of alloys. Adapted from Donachie et al Superalloys - A Technical Guide [8].

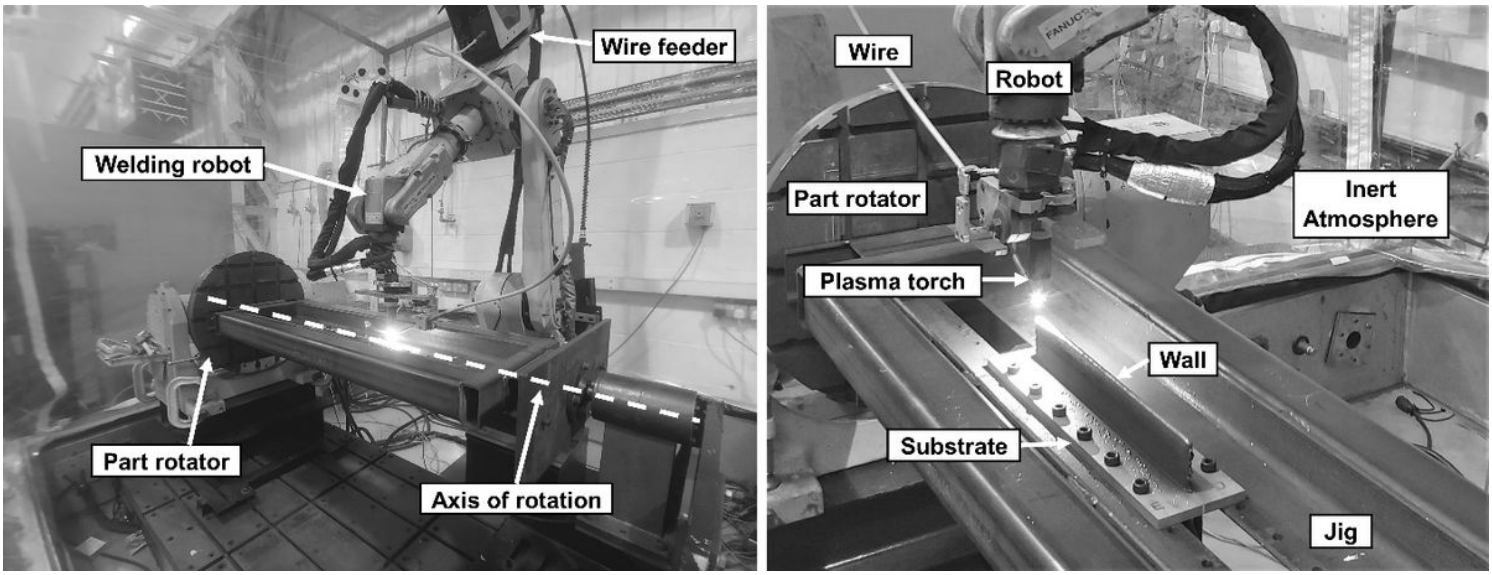

Figure 3

Experimental set-up for WAAM deposition.

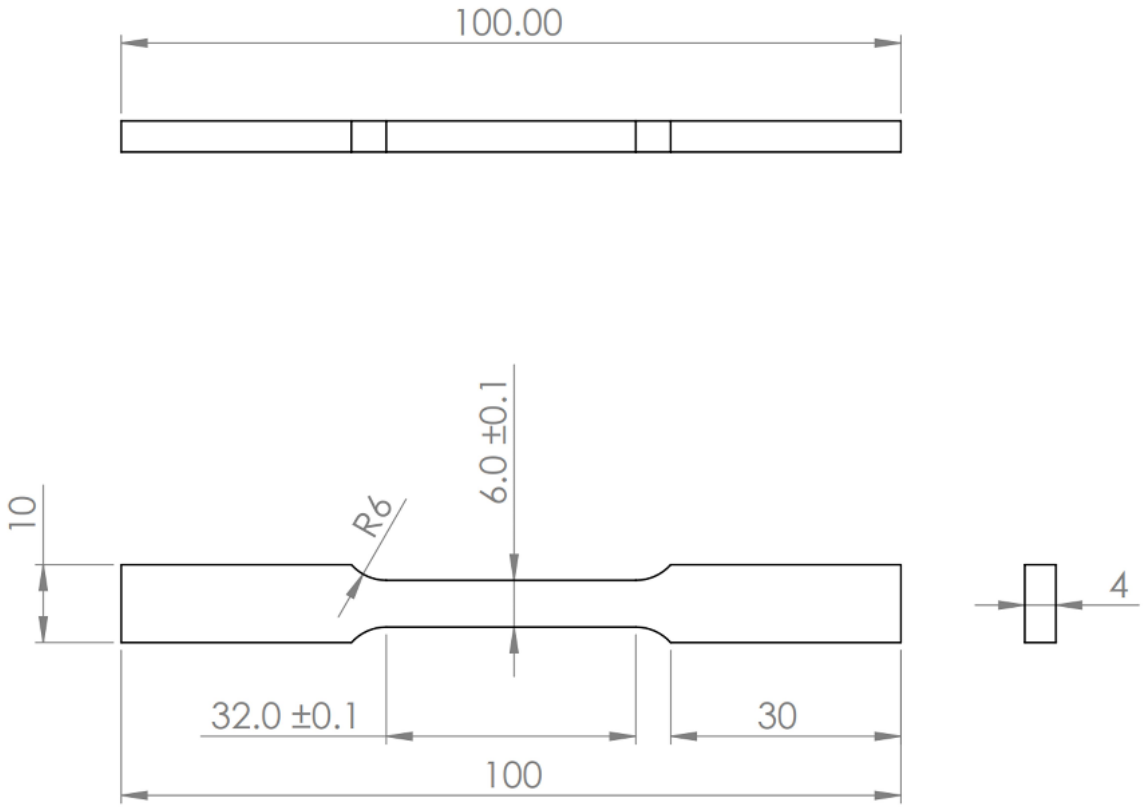

Figure 4

RT Tensile testing coupon. (Dimensions in mm).

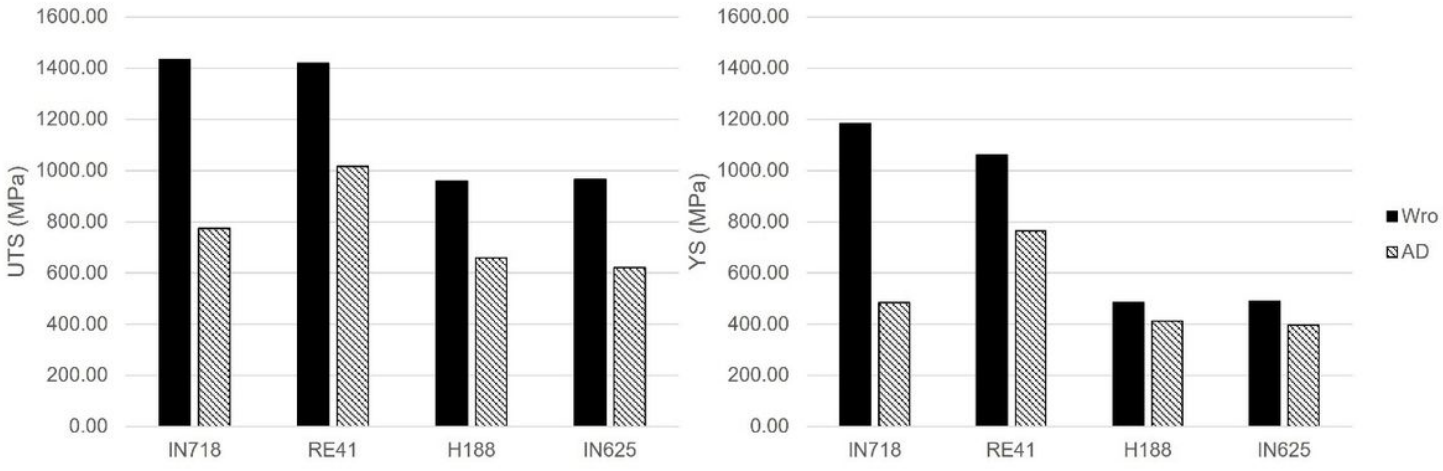

Figure 5

Graphical representation of data presented in Table 4.